







Article

# Microstructural and Mechanical Characterization of the Dissimilar AA7075 and AA2024 Aluminum Alloys Reinforced with Different Carbide Particles Welded by Friction Stir Welding

Essam B. Moustafa <sup>1,\*</sup> , Mazen Sharaf <sup>1</sup> , Ghazi Alsoruji <sup>1</sup> , Ahmed O. Mosleh <sup>2,\*</sup> , S. S. Mohamed <sup>2</sup>   
and Hossameldin Hussein <sup>3</sup> 

- <sup>1</sup> Mechanical Engineering Department, Faculty of Engineering, King Abdulaziz University, Jeddah 21589, Saudi Arabia; amazen@aljouf.com.sa (M.S.); gsaati@kau.edu.sa (G.A.)  
<sup>2</sup> Mechanical Engineering Department, Faculty of Engineering at Shoubra, Benha University, Cairo 11629, Egypt; samah.samir@feng.bu.edu.eg  
<sup>3</sup> Mechanical and Mechatronics Engineering Department, Higher Technological Institute, Tenth of Ramadan City 44637, Egypt; hossameldin@hti.edu.eg  
\* Correspondence: abmostafa@kau.edu.sa (E.B.M.); ahmed.omar@feng.bu.edu.eg (A.O.M.)

**Abstract:** In the present study, AA7075 and AA2024 aluminum alloys were reinforced with ZrC, and the particles of WC were joined using the friction stir welding (FSW) method. The microstructural and mechanical properties of the welds were investigated using SEM, EDS, and tensile tests. The FSW process resulted in high-quality welds with fine grain structure; the stirred zone has 666% smaller grain size than AA7075 and AA2024 aluminum alloys. The tensile test showed strong and ductile welds. The fracture test showed ductile and less brittle composite joints of AA2024 and AA7075 alloys reinforced with WC and ZrC. The processing parameters in the FSW process significantly affect tensile strength (UTS); therefore, the improvement of UTS with tool speed is much greater than with welding speed. Increasing the tool speed from 400 to 560 rpm increased UTS by 7.1%, and from 560 to 700 rpm by 5.4%. The tensile test results showed that the welds exhibited considerable strength and ductility. Fracture analysis showed that the composite joints made of different AA2024 and AA7075 alloys and reinforced with WC and ZrC were ductile and less brittle. This study showed that FSW can efficiently fuse different aluminum alloys reinforced with ceramic particles.

**Keywords:** FSW; mechanical properties; dissimilar alloy; composites; microstructure; zirconium carbide; tungsten carbide



**Citation:** Moustafa, E.B.; Sharaf, M.; Alsoruji, G.; Mosleh, A.O.; Mohamed, S.S.; Hussein, H. Microstructural and Mechanical Characterization of the Dissimilar AA7075 and AA2024 Aluminum Alloys Reinforced with Different Carbide Particles Welded by Friction Stir Welding. *J. Compos. Sci.* **2023**, *7*, 448. <https://doi.org/10.3390/jcs7110448>

Academic Editor: Francesco Tornabene

Received: 17 September 2023  
Revised: 4 October 2023  
Accepted: 12 October 2023  
Published: 30 October 2023



**Copyright:** © 2023 by the authors. Licensee MDPI, Basel, Switzerland. This article is an open access article distributed under the terms and conditions of the Creative Commons Attribution (CC BY) license (<https://creativecommons.org/licenses/by/4.0/>).

## 1. Introduction

The friction stir welding (FSW) technique is employed to fuse two or more materials, and involves the utilization of a rotating tool equipped with a specifically engineered pin inserted into the workpiece and traversed along the weld seam. The rotational tool generates frictional heat, causing the material to undergo plasticization. Simultaneously, the stirring action of the pin facilitates the mixing of the components [1,2]. Dissimilar aluminum composites are fabricated through the amalgamation of two or more distinct varieties of aluminum alloys. Various alloys can be selected to enhance the characteristics of the composite, including, but not limited to, strength, stiffness, and corrosion resistance [3–5]. The mechanical characteristics of dissimilar aluminum composites produced using FSW are influenced by many parameters: the selection of aluminum alloys, the manipulation of processing parameters (e.g., tool rotation speed, welding speed, and plunge depth), and the characterization of the resulting microstructure in the composite material [6–9]. The strength and stiffness of the composite material often exhibit enhanced

characteristics when the two constituent alloys possess comparable attributes [10,11]. However, using the FSW method to join plates that include ceramic particles raises concerns regarding the potential influence of these particles on the overall quality of the welds [12].

Incorporating ceramic particles within the welded plates can impact frictional heating and the resultant deformation behavior during welding. Therefore, the microstructure and mechanical qualities of the welds produced may experience alterations [13,14]. Based on empirical evidence, it has been shown that the inclusion of ceramic particles in the plates subjected to friction stir welding has a detrimental effect on both the tool's wear and the tensile strength of the resultant welds [15–17]. The effects of processing parameters on friction stir welding-made composite aluminum alloy connectors have been extensively studied [18–20]. Mechanical properties are affected by the composite's microstructure. The grain size and distribution of reinforcing particles in the matrix have a major impact on the strength and stiffness of a composite [21,22]. The augmented strength of composites can be primarily attributed to three key factors: grain refining, load transfer, and dislocation strengthening. Processing parameters affect the mechanical properties of friction stir welded (FSW) dissimilar aluminum composites, which have been extensively studied. Adjusting processing conditions improves composite mechanical characteristics, according to these investigations. An exemplary study examined how tool rotation speed affected the tensile strength and toughness of an aluminum alloy composite of AA2024 and AA7075 [23]. A separate investigation was conducted to examine the impact of welding speed on the tensile strength and hardness of a composite material composed of AA6061 and AA2024 aluminum alloys. The experimental findings indicated a positive correlation between the welding speed and the tensile strength and hardness of the composite material [24].

On the other hand, there has been a notable enhancement in the tensile strength of nanocomposites in recent times. The study conducted by [25] investigated the mechanical properties of a hybrid metal matrix composite consisting of an AA2024 alloy reinforced with silicon carbide (SiC) and fly ash. The findings unveiled a positive correlation between the rotational velocity of the tool and the tensile strength and toughness of the composite material. The tensile characteristics and low-cycle fatigue performance of two aluminum alloys, namely 10 vol% Al<sub>2</sub>O<sub>3</sub>-reinforced 7005 aluminum alloy and 20 vol% Al<sub>2</sub>O<sub>3</sub>-reinforced 6061 aluminum alloy, were evaluated by [26]. The study's findings indicated a positive correlation between the tool rotation speed and the tensile strength and toughness of the composite material. The aforementioned study, conducted by [27], reached a similar conclusion. As a result, their study was primarily concerned with evaluating the impact of B4C on the enhancement of mechanical properties in AA2014 aluminum matrix composites. The investigation results demonstrated a significant positive relationship between the tool's rotational velocity and the tensile strength and toughness of the composite material.

Previous research has demonstrated that the mechanical characteristics of dissimilar aluminum composites produced using friction stir welding (FSW) can be enhanced by optimizing processing parameters [28,29]. The aforementioned statement highlights the potential of FSW as a viable technique for the fusion of different aluminum alloys and for producing aluminum composites with enhanced performance [30]. The present investigation employed friction stir welding (FSW) to combine two different aluminum alloys, AA2024 and AA7075, previously reinforced with zirconium and tungsten carbides, respectively. The primary aim of this study is to determine the optimal processing parameters for friction stir welding to effectively combine two distinct composite materials. The utilization of friction stir welding (FSW) to join different aluminum alloys reinforced with ZrC and WC particles can be considered innovative. This is because FSW is a comparatively recent welding technique that has demonstrated its efficacy in joining many materials, including aluminum alloys.

Nevertheless, the current body of research regarding the utilization of friction stir welding (FSW) to join different aluminum alloys reinforced with carbide particles is quite scarce. Moreover, the present study is deemed innovative since it examines the impact of friction stir welding (FSW) on both the microstructure and mechanical properties of a

dissimilar junction composed of an aluminum alloy reinforced with ZrC and WC particles. The significance of this lies in the ability of FSW to introduce novel microstructural characteristics, such as shear bands and recrystallized grains, which can impact the mechanical properties of the welded joint.

The primary objective of this study was to achieve a high-quality weld with minimal or no flaws. The challenge arises from the amalgamation of dissimilar aluminum alloys, particularly when one incorporates ceramic reinforcements, resulting in complications such as porosity, cracks, and compromised mechanical characteristics. Examining and characterizing welding properties involves utilizing mechanical and microstructural analytical techniques. In addition, it is imperative to achieve precise control and optimization of processing parameters during friction stir welding of dissimilar metals reinforced with ZrC and WC particles.

## 2. Materials and Methods

In this study, AA2024 and AA7075 aluminum alloys were used as feedstocks, with zirconium carbide (ZrC) and tungsten carbide (WC) particles serving as reinforcing particles for friction stir welding (FSW). The chemical composition of the aluminum alloys was analyzed using a Founder-Master metal analyzer, as shown in Table 1. The literature highlights the distinguishing features of AA7075 and AA2024 aluminum alloys [14,31]. AA7075 is renowned for its notable strength and commendable resistance to fatigue, while it exhibits subpar corrosion resistance [32,33]. Conversely, AA2024 demonstrates high strength and commendable corrosion resistance, but its fatigue resistance is comparatively worse [34]. The reinforcement particles were examined by transmission electron microscopy (TEM), and the mean particle size was found to be less than 1  $\mu\text{m}$ , as shown in Figure 1. The friction stir welding (FSW) process was performed using a CNC milling machine, as shown in Figure 2a,b. The FSW tool was specially designed with a tapered triangular geometry, as shown in Figure 2c.

**Table 1.** The chemical composition of the dissimilar aluminum alloy and FSW tool K110 wt.%.

Aluminum Alloys	Cu	Zn	Si	Fe	Mg	Others	Al
AA2024	4.54	0.34	0.48	0.53	1.75	1.53	remain
AA7075	1.61	4.98	0.39	0.21	3.11	0.4	remain
FSP tool steel							
K110	C	Mn	Cr	V	Mo	Si	Fe
	1.55	0.75	11.3	0.75	0.75	0.3	Bal

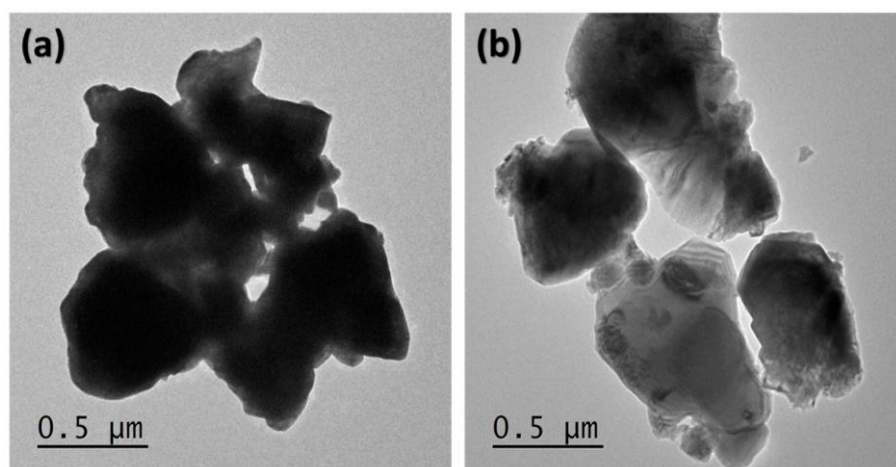


**Figure 1.** TEM images of the reinforcement particles (a) tungsten carbide, (b) zirconium carbide.

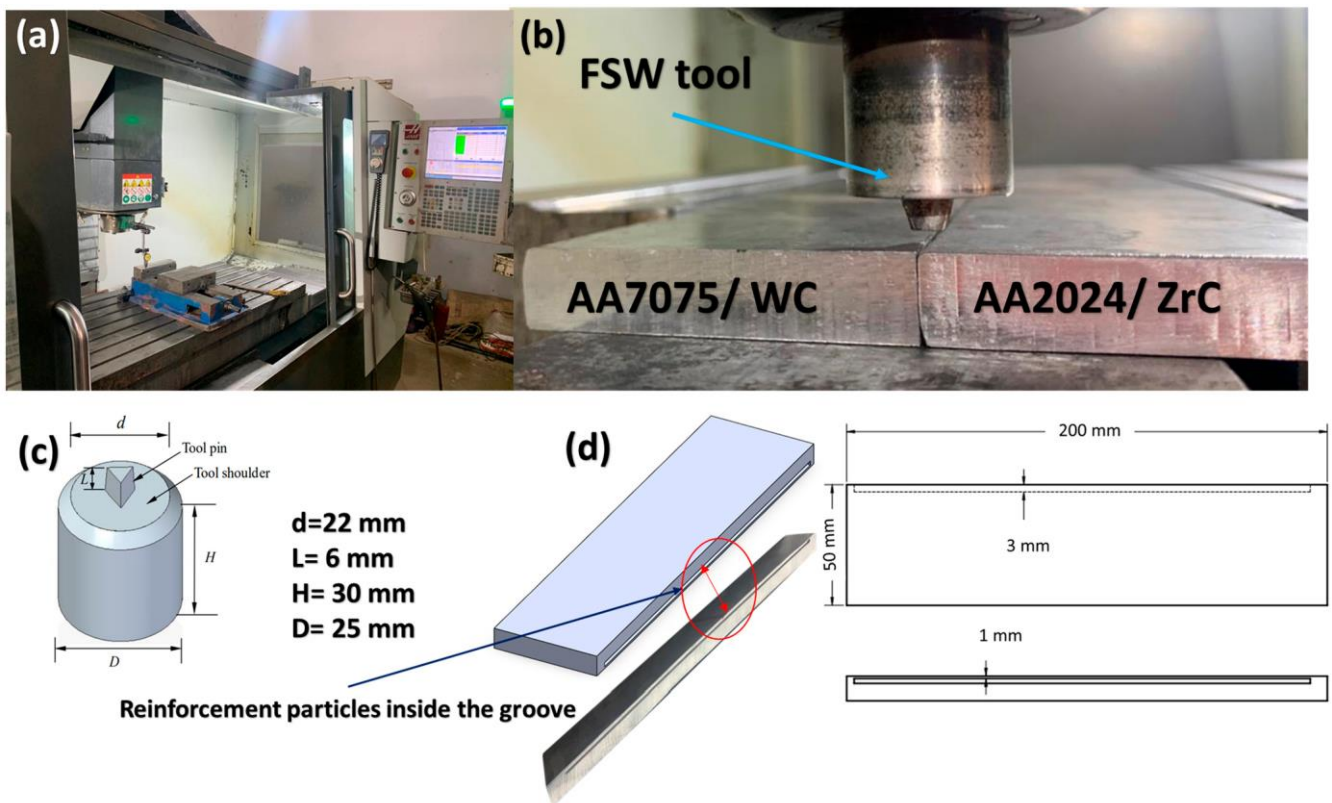


**Figure 2.** Friction stir welding FSW process, (a) CNC milling machine, (b) welding process, (c) FSW tool design, (d) groove design inside the welded sheet.

The aluminum sheets were machined and prepared using a computer numerically controlled (CNC) machine, and a longitudinal groove was milled into each sheet. The reinforcement particles were then placed in the grooves, as shown in Figure 2d. The rotational speeds of the tool were measured at 400, 560, and 700 revolutions per minute (rpm), while the traverse speeds were measured at 20, 25, and 30 mm per minute (mm/min). The welds were prepared for testing by using silicon carbide paper with different grit sizes, starting with 320 grit and gradually increasing to 2400 grit. The specimens were cooled with water, which removed loose metal particles and abrasive material. The specimens were etched with Keller's reagent, a conventional solution of 2 mL hydrofluoric acid (48%), 6 mL nitric acid, and 91 mL distilled water. This etching process is performed at room temperature for a short duration, usually a few seconds. The purpose of etching is to expose and examine the macro- and microstructure of the treated samples until the desired contrast is achieved. After the etching process, the samples were thoroughly cleaned. Tensile tests were performed to evaluate the mechanical properties of the specimens. To evaluate the tensile properties of the machined stirred zone, flat (dog bone) tensile specimens were taken from the central area of the machined zone and oriented parallel to the direction of machining, conforming to the American Society for Testing of Materials (ASTM) guidelines. A universal testing machine with a capacity of 300 kilonewtons was used to perform the tensile tests. The evaluation included the calculation of the modulus of elasticity, yield strength, ultimate tensile strength, and elongation. In addition, the specimens were analyzed using scanning electron microscopy (SEM). The actual phase composition and the reinforcement in the stirred zone were investigated using an X-ray diffraction approach in a Bruker D8 Advance diffractometer equipped with Cu-K radiation.



### 3. Results and Discussions

#### 3.1. Optical Microstructure Examination

Optical polarized light microscopy and scanning electron microscopy (SEM) were used to study the microstructural features of the stirring zone in different composite materials composed of AA2024 and AA7075 alloys reinforced with zirconium carbide (ZrC) and tungsten carbide (WC). Figure 3 shows optical micrographs of the AA7075 and AA2024 aluminum alloys, showing average grain sizes of  $80 \pm 5 \mu\text{m}$  and  $180 \pm 10 \mu\text{m}$ , respectively. In addition, the figure shows the stirred zone (SZ), heat affected zone (HAZ), and thermomechanically affected zone (TMHAZ) in a friction stir welded joint. Alloy AA7075 exhibits a coarse-grained microstructure, as shown in Figure 3a. Similarly, alloy AA2024 exhibits a coarser rolled grain microstructure, as shown in Figure 3b.

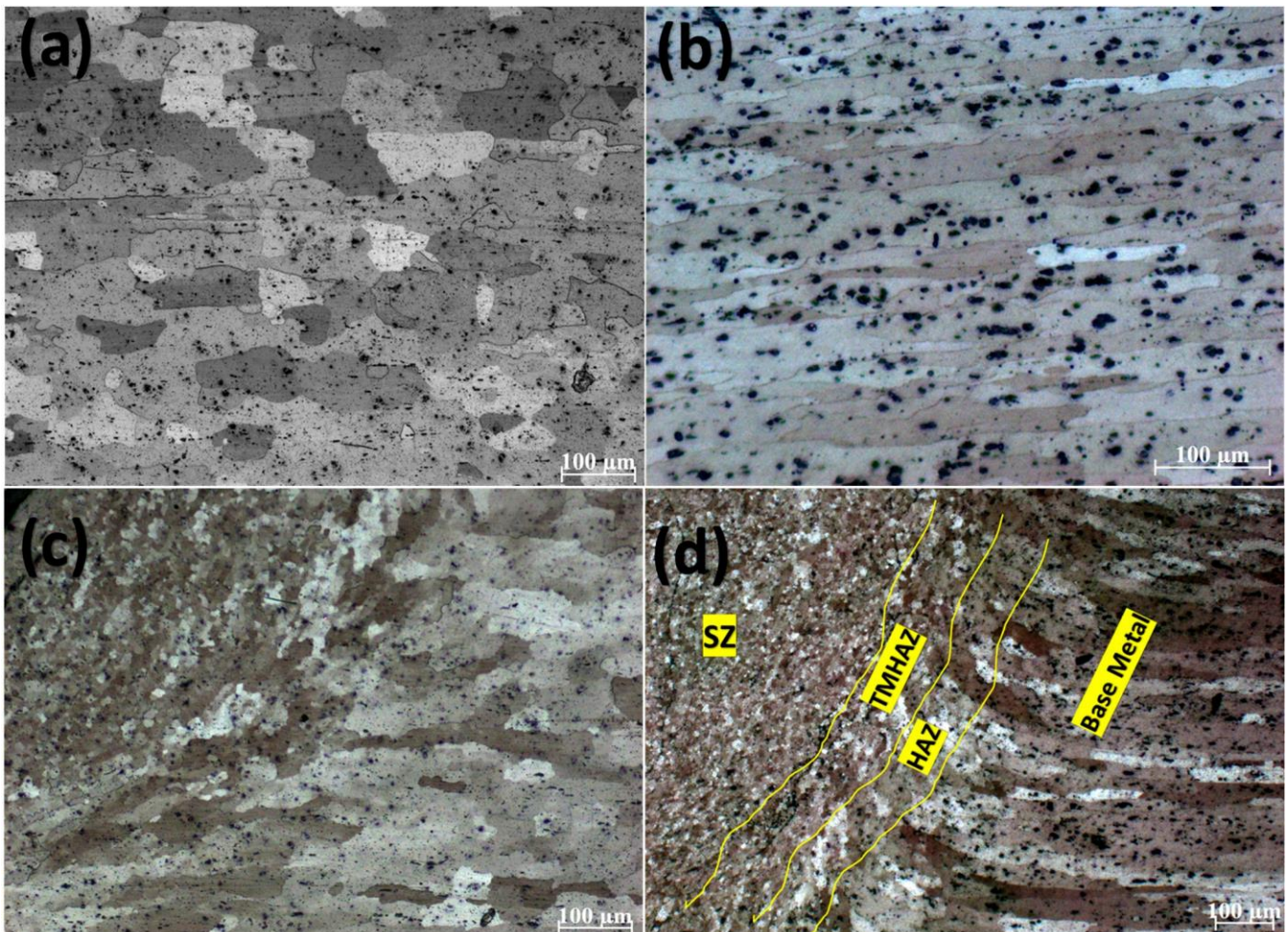


**Figure 3.** Optical microscopy images of the investigated alloys, (a) AA7075 aluminum alloy, (b) AA2024 aluminum alloy, (c) different zones SZ, HAZ, TMHAZ, and base metals near AA7075 metal, (d) different zones SZ, HAZ, TMHAZ, and base metals near from AA2024 metal.

The heat-affected zone (HAZ) refers to the weld area that has been thermally affected by the welding process but has not completely melted. The thermomechanically affected zone (TMHAZ) is the area of the weld that has been affected by the heat and mechanical forces of the welding process. It is characterized by a distorted grain structure (Figure 3c,d). The different areas of the weld can be distinguished by their various microstructural features. The tiny equiaxed grain structure in the stirred zone results from the constituents' melting and mixing process. The heat generated during welding results in a coarser grain structure in the heat-affected zone (HAZ). The grain structure of the TMHAZ exhibits

deformation due to the thermal and mechanical effects during the welding process. Figure 4 shows the stirred zone of the mixed materials; according to this figure, the average grain size was refined to  $12 \pm 4 \mu\text{m}$ , characterized by a fine equiaxed grain structure.



**Figure 4.** The stirred zone image inside the welded joint is in the middle position of the welded joint.

The experimental results indicate that an optimum weld zone was achieved with a higher tool speed and a moderate traverse speed. The welding parameters used in this study resulted in a microstructure without defects and a homogeneous distribution of reinforcement particles. In addition, the grain structure was refined, resulting in a more uniform dispersion. The uniform dispersion of the reinforcement particles was identified as the cause of the decrease in grain size and the improvement in mechanical properties in the stirred zone. The rotational speed of the tool was found to have a significant effect on the microstructure of the welded joints. At higher rotational speeds, the ZrC and WC particles were more evenly distributed in the joint, resulting in a finer and more uniform microstructure.

In contrast, the particles agglomerated at lower speeds were unevenly distributed in the joint, resulting in a coarser microstructure. In addition, the travel speed also played a crucial role in determining the microstructure and mechanical properties of the joints. The material experiences lower heat input and shorter cooling times at higher travel speeds, resulting in a finer microstructure with smaller particles. Lower travel speeds, on the other hand, resulted in a coarser microstructure with larger particles.

The different areas of the weld can be distinguished by their different microstructural features. The tiny equiaxed grain structure in the stirred zone results from the constituents' melting and mixing process. The heat generated during welding results in a coarser grain structure in the heat-affected zone (HAZ). The grain structure of the TMHAZ exhibits deformation due to the thermal and mechanical influences during the welding process. A lower tool welding speed also gives the particles more time to disperse before welding. The SEM images of the joints (Figure 5) show a uniform distribution of the reinforcement particles within the stirred zone. This is due to the high heat energy in the weld zone, which helps to break up and evenly distribute the particles. The welding process is not as efficient at lower speeds, and the particles are not as well distributed. This can lead to defects and voids in the weld. For example, the weld quality deteriorated when the tool speed was reduced to 400 rpm while maintaining a travel speed of 30 mm/min (Figure 6). This was because the reduced heat input hindered the adequate fusion and homogenization of the materials. The EDX data from the SEM image illustrates the relationship between each element's weight and atomic percentage inside the composites that friction stir welding



(FSW) produces. The weight percentage of zirconium carbide (ZrC) is 0.06%, while the atomic percentage is 0.02%. The weight percentage of tungsten carbide (WC) is 10.42%, while the atomic percentage is 1.73%. The findings of this study suggest that the composites produced by friction stir welding (FSW) contain ZrC and WC; however, their presence is observed to be rather limited. Its high hardness and brittleness characterize zirconium carbide (ZrC), whereas tungsten carbide (WC) exhibits exceptional hardness and wear resistance properties. Including these materials in the composites leads to enhancements in the mechanical properties.

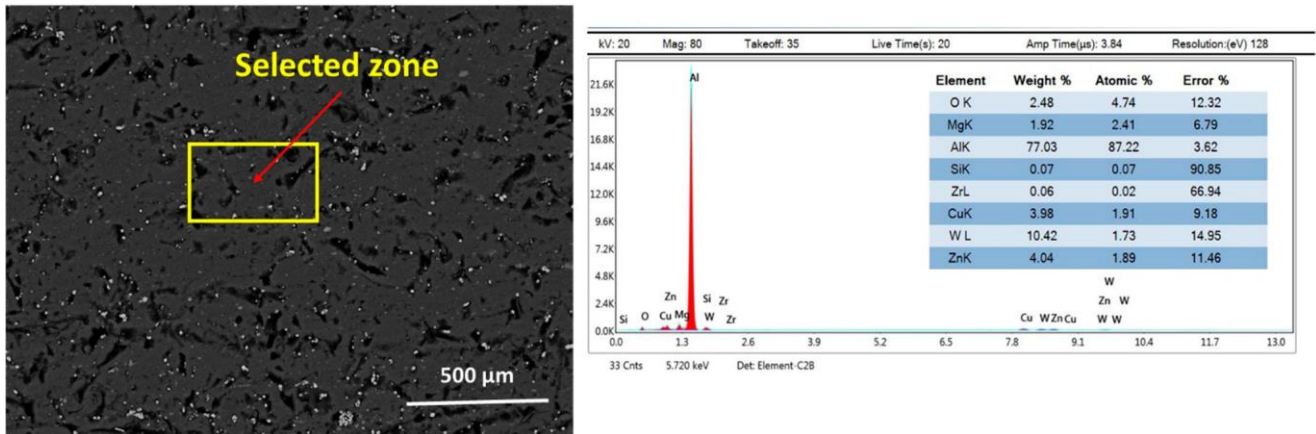


Figure 5. SEM image of the FSW joint processed at 700 rpm tool rotation speed and 20 mm/min welding speed.

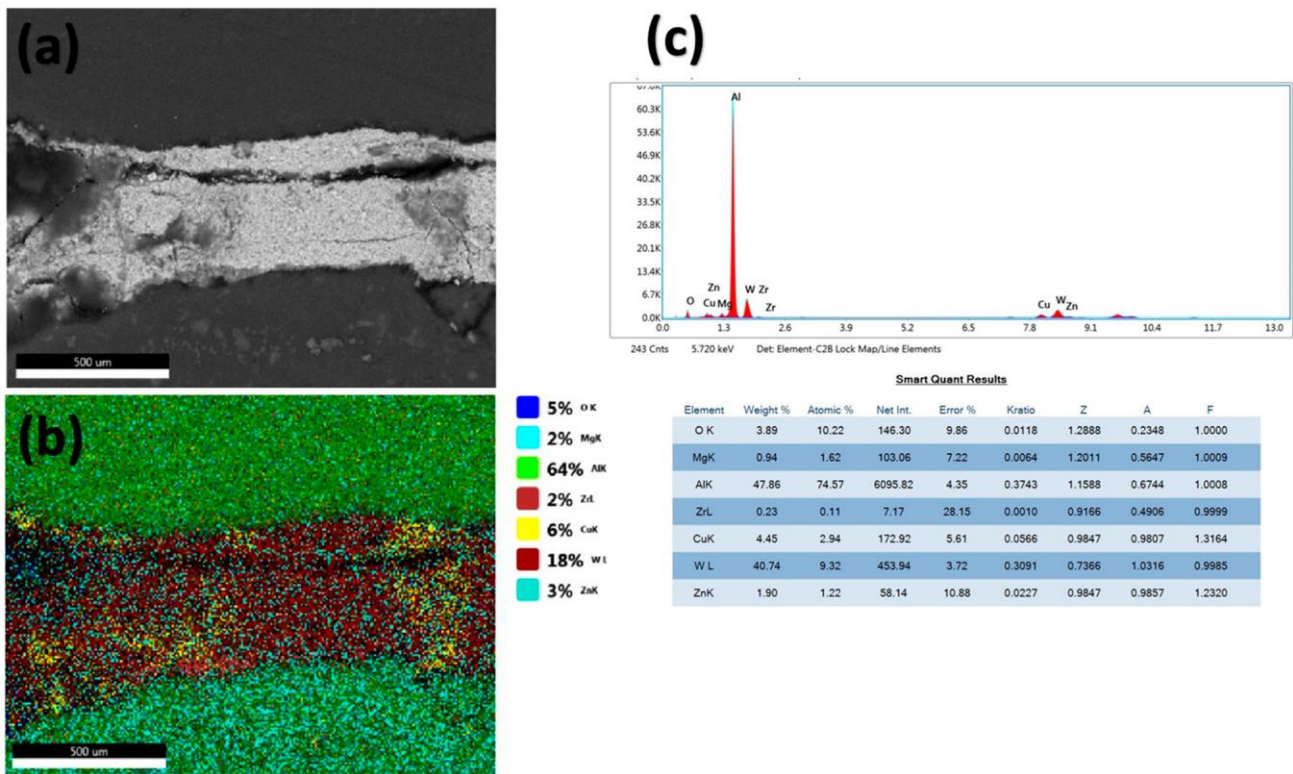
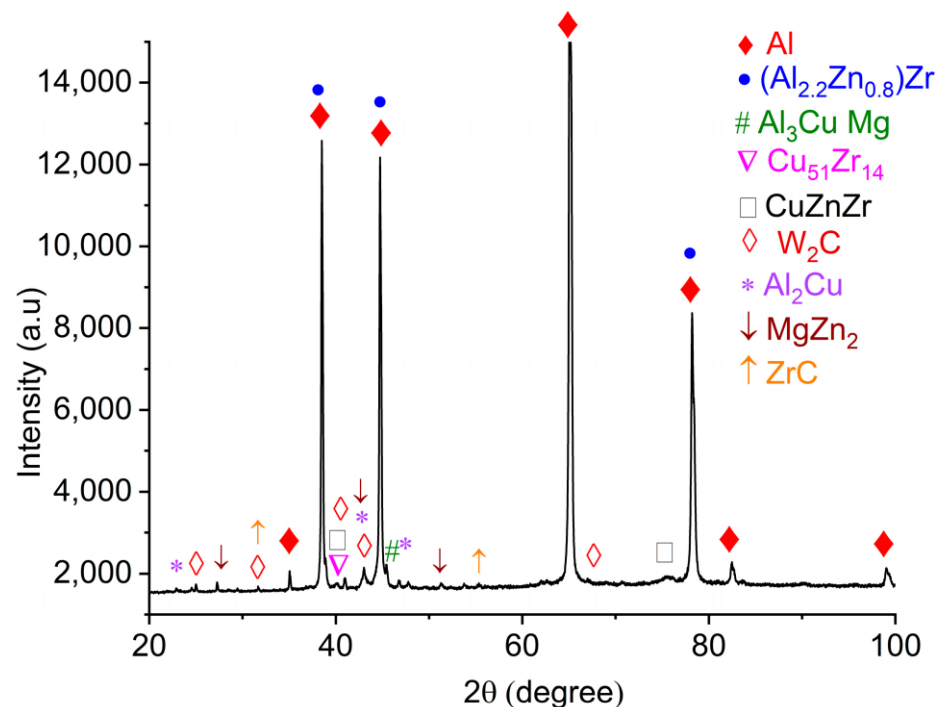


Figure 6. SEM image of the FSW mid-joint of the samples processed at 400 rpm and 20 mm/min processing parameter (a) typical SEM microstructure, (b) elemental mapping of the reinforcement and alloying element distribution, (c) EDX analysis summarizes the results of an energy dispersive X-ray (EDX) analysis.

The results show that tool speed and tool welding speed are important factors to consider in friction stir welding materials with reinforcement particles. By optimizing these parameters, it is possible to achieve better particle distribution and a more uniform weld. Higher rotational speeds, on the other hand, generate more heat and turbulence, which help to break up the particles and distribute them more evenly. This results in better dispersion of the particles and a more uniform weld.

### 3.2. Phase Composition

X-ray diffraction (XRD) determined the samples' phase composition. The X-ray diffraction pattern of the weld shown in Figure 7 shows distinct peaks at 38.51°, 44.68°, 65.21°, and 78.12°. These peaks indicate the presence of aluminum (Al) and  $(Al_{2.2}Zn_{0.8})Zr$  in the joint. From the ICCD maps 89-1981 and 28-0014, it can be deduced that the observed peaks at 43.52° and 48.04° correspond to the intermetallic phases  $Al_2Cu$  and  $Al_3CuMg$ , respectively. The above phases are coarse precipitates that have not dissolved and are distributed over the grain boundaries of the underlying alloy. The formation of  $AlCuMg$  precipitates in the stir zone of a friction stir welded joint can increase the strength and ductility of the joint [35]. However, this is not the case if the welding temperature is too high.



**Figure 7.** The XRD patterns of the welded zone.

In this case,  $Al_2Cu$  may be formed in the metal matrix, which decreases the strength and ductility of the joint, and this intermetallic compound appears in small amounts in the XRD image. For example, the decay of  $Al_2Cu$  particles can lead to a decrease in hardness and wear resistance. On the other hand, the accumulation of  $Al_2Cu$  particles can increase hardness and wear resistance [36]. The influence of newly developed precipitates on the tribological properties of aluminum composites is of great importance [37]. The observation of the  $W_2C$  phase is also evident in the (XRD) pattern of the hybrid composite. The use of ceramics in the (FSW) process leads to a decrease in crystal size and an increase in the dislocation density of the aluminum tips, as shown by the (XRD) analysis. This effect is particularly evident in samples containing hybrid reinforcement. The observed behavior can be attributed to the improved refinement of the aluminum grains resulting from the inclusion of ceramic elements. The dissolution and deposition of reinforcement particles can significantly affect the tribological properties of aluminum composites.



### 3.3. Mechanical Properties

The mechanical properties of FSW joints are subject to the influence of various elements, such as the properties of the reinforcing particles (e.g., type and size), the volume fraction of the particles, and the processing parameters. Usually, an increase in the volume fraction of the particles leads to a corresponding improvement in the mechanical properties. However, the optimum volume fraction depends on the specific application. The mechanical properties of FSW joints are significantly influenced by two critical production parameters: welding and tool speed. The speed at which welding is performed directly affects the amount of heat transferred to the joint, thus influencing the grain size and microstructure of the joint. A higher welding speed is associated with a smaller grain size and a more uniform microstructure, which can improve the mechanical properties of the weld. The device's rotational speed significantly affects the agitation mechanism, facilitating the joint's uniform distribution of reinforcement particles. Increasing the rotation speed of the device leads to a more homogeneous distribution of the particles, which can improve the mechanical properties of the joint. The results of the tensile tests performed on the studied specimens at different tool rotational speeds and welding speeds are shown in Figure 8.

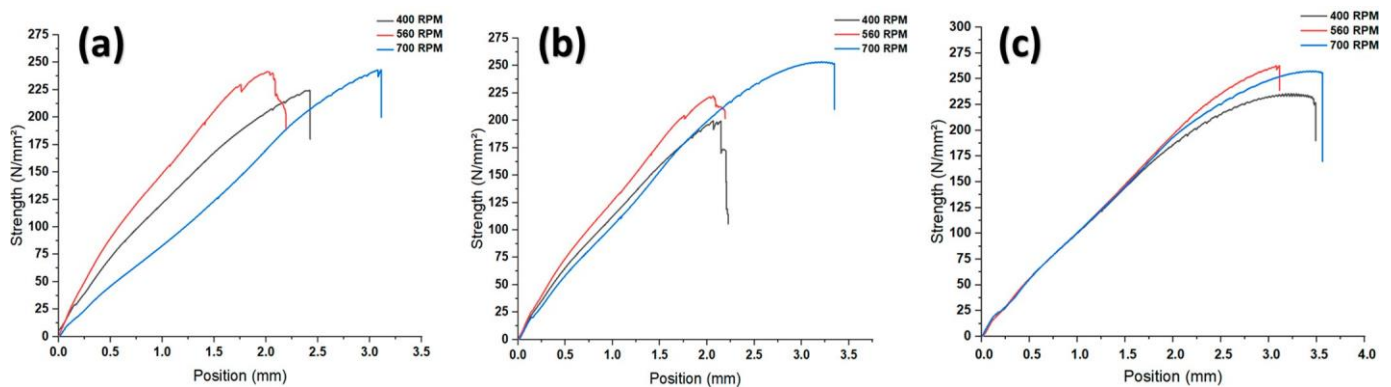


**Figure 8.** Tensile test results of the investigated samples at different tool rotation speeds and welding speeds. (a) Traverse speed 20 mm/min, (b) 25 mm/min, (c) 30 mm/min.

The observed trend shows a positive correlation between the tool speed and the tensile strength (UTS). This phenomenon can be attributed to the increased heat energy generated in the stirred zone (SZ) when the tool rotation speed increases. The increased heat input facilitates dynamic recrystallization (DRX) in the SZ, a phenomenon that leads to the refinement of the grain structure and an increase in material strength. Using DRX also helps reduce voids within the SZ, further increasing tensile strength (UTS). The study found a positive correlation between tool speed and tensile strength (UTS). However, the effect of welding speed on UTS was rather small. The optimum tool rotation and welding speed combination depends on the composite material being welded.

Friction stir welding (FSW) of composites affects tensile strength (UTS), as shown in Figure 9. The results show that the UTS of FSW composites improves with increasing tool speed. Welding speeds of 20, 25, and 30 mm/min resulted in UTS values of 224 MPa, 198 MPa, and 235 MPa, respectively, when evaluated at a tool speed of 400 rpm. Tensile strengths (UTS) of 240 MPa, 222 MPa, and 262 MPa were measured at welding speeds of 20, 25, and 30 mm/min, respectively, and at a speed of 560 rpm. We found that the UTS values for welding speeds of 20, 25, and 30 mm/min were 242 MPa, 253 MPa, and 257 MPa, respectively, when the tool speed reached 700 rpm. From the results, it can be concluded that the tool speed is the most important factor in determining the UTS of the friction stir welded composite. Although the welding speed slightly increases UTS, its influence on the final product is negligible. The ideal turning and welding speeds vary depending on the weld material's properties. The maximum tensile strength (UTS) was achieved with a tool speed of 700 rpm and a welding speed of 25 mm/min, as determined in this study.

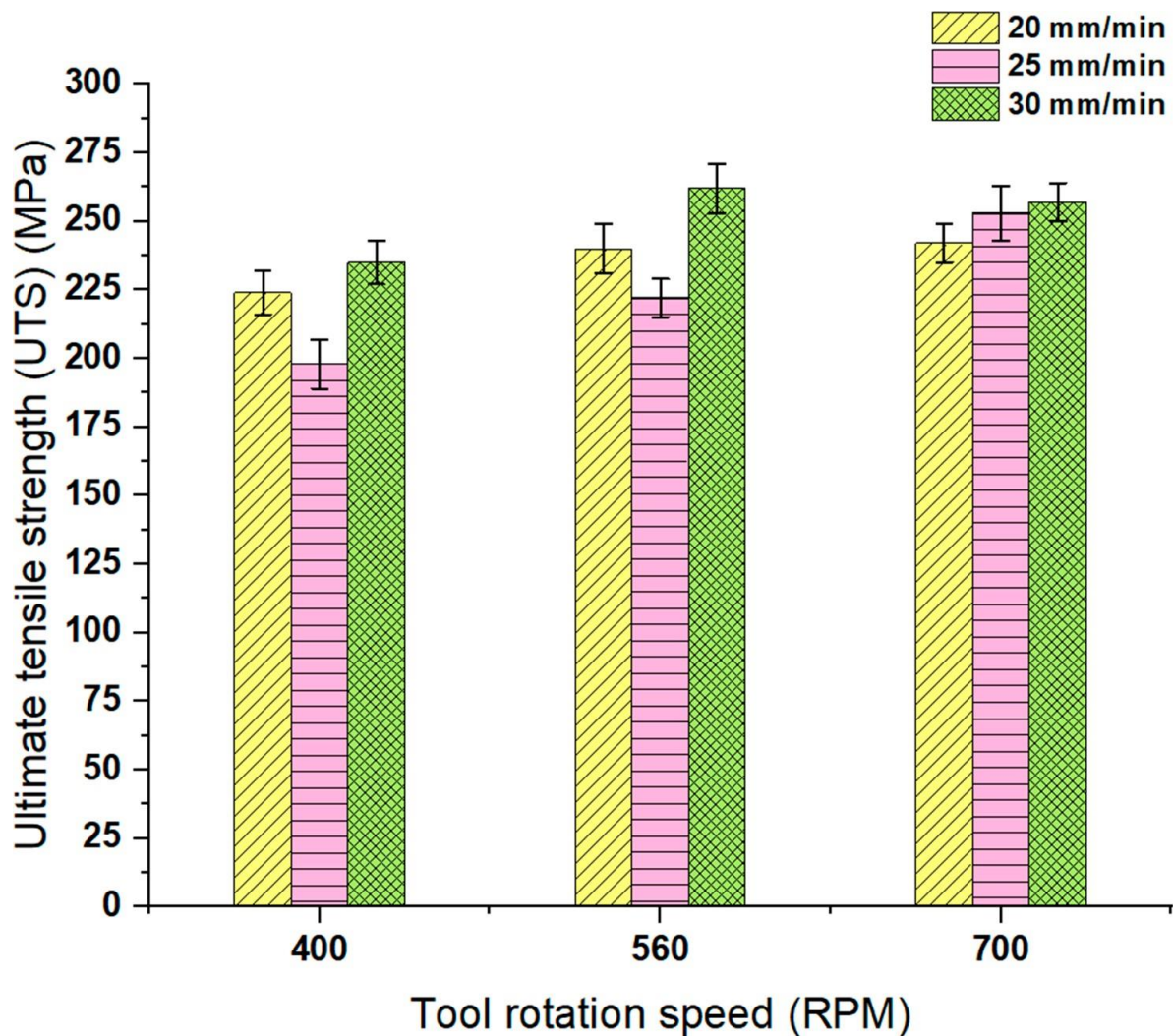


**Figure 9.** Effect of tool rotation speed on ultimate tensile strength of friction stir welded composite.

### 3.4. Fracture Analysis

The fracture analysis of specimens from the tensile test performed on the composite joints of AA2024 and AA7075 alloys reinforced with WC and ZrC was performed by scanning electron microscopy (SEM). The samples were recorded and examined before the examination (SEM), as shown in Figure 10. This was carried out to anticipate and understand the behavior of the fracture mechanism. Fracture analysis within the gage length center is generally characterized by ductile behavior. This means significant plastic deformation occurs before the material reaches its fracture point. SEM is a technique that uses an electron beam to image the surface of a material. Images from SEM show that the fracture surfaces of the specimens have various features, including pits, cracks, and shear lips. The dimples were the predominant feature on the fracture surfaces, indicating that the specimens were fractured in a ductile manner (Figure 11a). The images from SEM also show that the fractured surfaces of the specimens were covered with a debris layer. Figure 11b shows some small cracks found in the examined images. There are many reasons for these cracks, e.g., the considerable thermal residual stresses in the weld area, which increase the probability of crack formation [38].

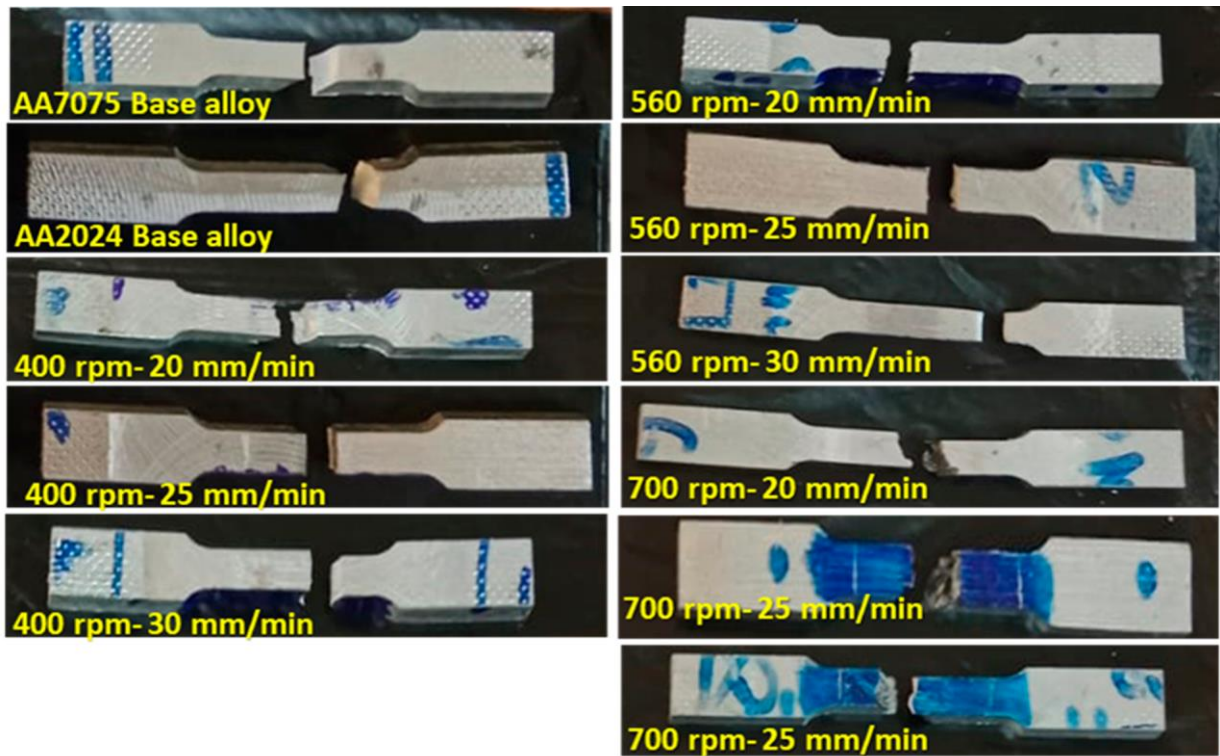


**Figure 10.** Fracture position of the investigated samples after tensile test at different tool rotation and welding speeds.

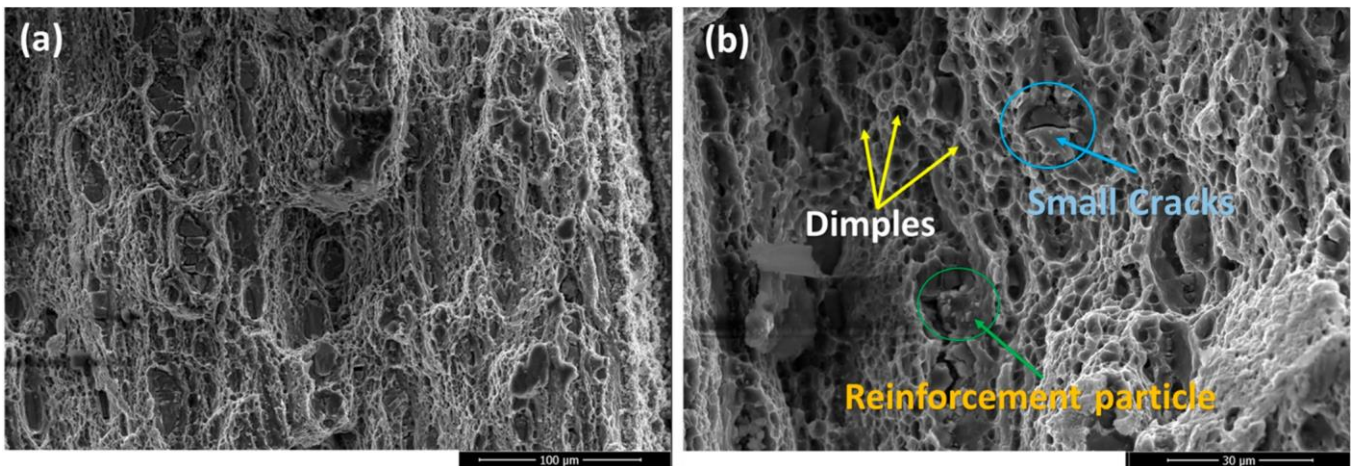


**Figure 11.** SEM images showing (a) ductile fracture showing dimple distribution and (b) higher magnification topographic features showing details of dimples and intermetallic compounds, as the reinforcement particles, the samples for joint welded at processing parameters of 700 rpm and 25 mm/min.

The dissimilar aluminum alloys AA2024 and AA7075 have different material properties, making them susceptible to fracture. For example, AA7075 had a higher degree of brittleness than AA2024, making it more susceptible to fracture when subjected to external mechanical loading [39]. Using incorrect welding parameters in friction stir welding can affect the quality of the weld and increase the likelihood of cracking. This is the case, for example, if an excessively high welding speed is used, which can increase the probability of thermal cracking [40]. In addition to the above features, the SEM images showed the presence of WC and ZrC particles on the fracture surfaces. These particles were embedded in the aluminum matrix and were not fractured. The results of the fracture analysis show



that the composite joints of the dissimilar alloys AA2024 and AA7075 reinforced with WC and ZrC have good ductility and are less likely to be brittle.

#### 4. Conclusions

This work successfully used friction stir welding (FSW) to join two dissimilar aluminum alloys, AA2024 and AA7075. The welding parameters significantly impact the quality of the welded joint.

The FSW process refines the grain structure in the stir zone, the weld region that is heated and mixed by the welding tool. The average grain size in the stir zone was reduced from 180  $\mu\text{m}$  to 12  $\mu\text{m}$ .

The ultimate tensile strength (UTS) of the FSW joint increased by 7.1% when the tool rotation speed was increased from 400 rpm to 560 rpm and by 5.4% when the tool rotation speed was further increased from 560 rpm to 700 rpm. The UTS also increased slightly as the welding speed increased, but the improvement was not as significant as the improvement due to tool rotation speed.

The presence of AlCuMg precipitates in the stir zone can improve the strength and ductility of the joint. However, if the welding temperature is too high, intermetallic compounds (IMCs) such as Al<sub>2</sub>Cu can form, reducing the joint's strength and ductility.

The fracture surfaces of the FSW joints exhibited a dimpled morphology, indicating that the samples underwent ductile fracture. Overall, the results of this study suggest that FSW is a promising technique for joining dissimilar aluminum alloys.

**Author Contributions:** Conceptualization, E.B.M., M.S. and A.O.M.; methodology E.B.M., M.S. and A.O.M.; software, A.O.M.; validation, E.B.M., M.S. and A.O.M.; formal analysis, E.B.M., A.O.M. and H.H.; investigation, A.O.M.; resources, G.A.; data curation, H.H. and E.B.M.; writing—original draft preparation, M.S. and A.O.M.; writing—review and editing, E.B.M.; visualization, S.S.M. and H.H.; supervision, E.B.M. and A.O.M. All authors have read and agreed to the published version of the manuscript.

**Funding:** This research received no external funding.

**Data Availability Statement:** Not applicable.

**Conflicts of Interest:** The authors declare no conflict of interest.

#### References

1. Zhang, Y.N.; Cao, X.; Larose, S.; Wanjara, P. Review of tools for friction stir welding and processing. *Can. Metall. Q.* **2012**, *51*, 250–261. [[CrossRef](#)]
2. Malik, V.; Sanjeev, N.K.; Hebbar, H.S.; Kailas, S.V. Investigations on the Effect of Various Tool Pin Profiles in Friction Stir Welding Using Finite Element Simulations. *Procedia Eng.* **2014**, *97*, 1060–1068. [[CrossRef](#)]
3. Moreira, F.; Ferreira, P.M.; Silva, R.J.C.; Santos, T.G.; Vidal, C. Aluminium-Based Dissimilar Alloys Surface Composites Reinforced with Functional Microparticles Produced by Upward Friction Stir Processing. *Coatings* **2023**, *13*, 962. [[CrossRef](#)]
4. Singh, H.; Dhindaw, B.K. Metal Matrix Composites: Aluminum. In *Wiley Encyclopedia of Composites*; Wiley: Hoboken, NJ, USA, 2012; pp. 1–18.
5. Shrivastava, S.P.; Agrawal, G.K.; Nagpal, S.; Vishvakarma, A.K.; Khandelwal, A.K. Dissimilar aluminum alloy joint strength is effected by heat addition in friction stir welding (FSW). *Mater. Today Proc.* **2021**, *44*, 1472–1477. [[CrossRef](#)]
6. Jabraeili, R.; Jafarian, H.R.; Khajeh, R.; Park, N.; Kim, Y.; Heidarzadeh, A.; Eivani, A.R. Effect of FSW process parameters on microstructure and mechanical properties of the dissimilar AA2024 Al alloy and 304 stainless steel joints. *Mater. Sci. Eng. A* **2021**, *814*, 140981. [[CrossRef](#)]
7. Abd Elnabi, M.M.; Elshalakany, A.B.; Abdel-Mottaleb, M.M.; Osman, T.A.; El Mokadem, A. Influence of friction stir welding parameters on metallurgical and mechanical properties of dissimilar AA5454–AA7075 aluminum alloys. *J. Mater. Res. Technol.* **2019**, *8*, 1684–1693. [[CrossRef](#)]
8. Dinaharan, I.; Kalaiselvan, K.; Vijay, S.J.; Raja, P. Effect of material location and tool rotational speed on microstructure and tensile strength of dissimilar friction stir welded aluminum alloys. *Arch. Civ. Mech. Eng.* **2012**, *12*, 446–454. [[CrossRef](#)]
9. Dorbane, A.; Mansoor, B.; Ayoub, G.; Shunmugasamy, V.C.; Imad, A. Mechanical, microstructural and fracture properties of dissimilar welds produced by friction stir welding of AZ31B and Al6061. *Mater. Sci. Eng. A* **2016**, *651*, 720–733. [[CrossRef](#)]
10. Siddharthan, B.; Rajiev, R.; Saravanan, S.; Naveen, T.K. Effect of Silicon Carbide in Mechanical Properties of Aluminium Alloy Based Metal Matrix Composites. *IOP Conf. Ser. Mater. Sci. Eng.* **2020**, *764*, 012040. [[CrossRef](#)]

11. Moustafa, E.B.; Taha, M.A. The Effect of Mono and Hybrid Additives of Ceramic Nanoparticles on the Tribological Behavior and Mechanical Characteristics of an Al-Based Composite Matrix Produced by Friction Stir Processing. *Nanomaterials* **2023**, *13*, 2148. [[CrossRef](#)]
12. Gibson, B.T.; Lammlein, D.H.; Prater, T.J.; Longhurst, W.R.; Cox, C.D.; Ballun, M.C.; Dharmaraj, K.J.; Cook, G.E.; Strauss, A.M. Friction stir welding: Process, automation, and control. *J. Manuf. Process.* **2014**, *16*, 56–73. [[CrossRef](#)]
13. Mirjavadi, S.S.; Alipour, M.; Emamian, S.; Kord, S.; Hamouda, A.M.S.; Koppad, P.G.; Keshavamurthy, R. Influence of TiO<sub>2</sub> nanoparticles incorporation to friction stir welded 5083 aluminum alloy on the microstructure, mechanical properties and wear resistance. *J. Alloys Compd.* **2017**, *712*, 795–803. [[CrossRef](#)]
14. Moustafa, E. Effect of Multi-Pass Friction Stir Processing on Mechanical Properties for AA2024/Al<sub>2</sub>O<sub>3</sub> Nanocomposites. *Materials* **2017**, *10*, 1053. [[CrossRef](#)] [[PubMed](#)]
15. Cioffi, F.; Fernández, R.; Gesto, D.; Rey, P.; Verdera, D.; González-Doncel, G. Friction stir welding of thick plates of aluminum alloy matrix composite with a high volume fraction of ceramic reinforcement. *Compos. Part A Appl. Sci. Manuf.* **2013**, *54*, 117–123. [[CrossRef](#)]
16. Abnar, B.; Gashtiazar, S.; Javidani, M. Friction Stir Welding of Non-Heat Treatable Al Alloys: Challenges and Improvements Opportunities. *Crystals* **2023**, *13*, 576. [[CrossRef](#)]
17. Kundu, A.K.; Gupta, M.K.; Rajput, N.S.; Rathore, R. Adhesive assisted TiB<sub>2</sub> coating effects on friction stir welded joints. *Sci. Rep.* **2022**, *12*, 17894. [[CrossRef](#)]
18. Hassanifard, S.; Ghiasvand, A.; Hashemi, S.M.; Varvani-Farahani, A. The effect of the friction stir welding tool shape on tensile properties of welded Al 6061-T6 joints. *Mater. Today Commun.* **2022**, *31*, 103457. [[CrossRef](#)]
19. Rudrapati, R. Effects of welding process conditions on friction stir welding of polymer composites: A review. *Compos. Part C Open Access* **2022**, *8*, 100269. [[CrossRef](#)]
20. Abdel Aziz, S.S.; Abulkhair, H.; Moustafa, E.B. Role of hybrid nanoparticles on thermal, electrical conductivity, microstructure, and hardness behavior of nanocomposite matrix. *J. Mater. Res. Technol.* **2021**, *13*, 1275–1284. [[CrossRef](#)]
21. He, T.; Ertuğrul, O.; Ciftci, N.; Uhlenwinkel, V.; Nielsch, K.; Scudino, S. Effect of particle size ratio on microstructure and mechanical properties of aluminum matrix composites reinforced with Zr<sub>48</sub>Cu<sub>36</sub>Ag<sub>8</sub>Al<sub>8</sub> metallic glass particles. *Mater. Sci. Eng. A* **2019**, *742*, 517–525. [[CrossRef](#)]
22. Hassan, A.S.; Moustafa, E.B.; Mohamed, S.S. Impact of welding processing parameters on the microstructure grain refinement and hardness behavior of the aluminum AA1050 joints. *Egypt. J. Chem.* **2023**, *66*, 291–302. [[CrossRef](#)]
23. Padmanaban, R.; Balusamy, V.; Vaira Vignesh, R. Effect of friction stir welding process parameters on the tensile strength of dissimilar aluminum alloy AA2024-T3 and AA7075-T6 joints. *Mater. Werkst.* **2020**, *51*, 17–27. [[CrossRef](#)]
24. Devaraju, A.; Jeshrun Shalem, M.; Manichandra, B. Effect of Rotation speed on Tensile Properties & Microhardness of Dissimilar Al Alloys 6061-T6 to 2024-T6 Welded via Solid State Joining Technique. *Mater. Today Proc.* **2019**, *18*, 3286–3290. [[CrossRef](#)]
25. Boopathi, M.; Arulshri, K.P.; Iyandurai, N. Evaluation of Mechanical Properties of Aluminium Alloy 2024 Reinforced with Silicon Carbide and Fly Ash Hybrid Metal Matrix Composites. *Am. J. Appl. Sci.* **2013**, *10*, 219–229. [[CrossRef](#)]
26. Ceschini, L.; Minak, G.; Morri, A. Tensile and fatigue properties of the AA6061/20vol% Al<sub>2</sub>O<sub>3</sub>p and AA7005/10vol% Al<sub>2</sub>O<sub>3</sub>p composites. *Compos. Sci. Technol.* **2006**, *66*, 333–342. [[CrossRef](#)]
27. Kara, M.; Coskun, T.; Gunoz, A. Influence of B4C on enhancing mechanical properties of AA2014 aluminum matrix composites. *Proc. Inst. Mech. Eng. Part C J. Mech. Eng. Sci.* **2021**, *236*, 2536–2545. [[CrossRef](#)]
28. Uday, K.N.; Rajamurugan, G. Influence of process parameters and its effects on friction stir welding of dissimilar aluminium alloy and its composites—A review. *J. Adhes. Sci. Technol.* **2023**, *37*, 767–800. [[CrossRef](#)]
29. Pookamnerd, Y.; Thosa, P.; Charonerat, S.; Prasomthong, S. Development of mechanical property prediction model and optimization for dissimilar aluminum alloy joints with the friction stir welding (FSW) process. *EUREKA Phys. Eng.* **2023**, *3*, 112–128. [[CrossRef](#)]
30. Dahiya, M.S.; Kumar, V.; Verma, S. A Critical Review on Friction Stir Welding of Dissimilar Aluminium Alloys. In Proceedings of the Advances in Industrial and Production Engineering, Singapore, 24 April 2019; pp. 707–719.
31. Khoshaim, A.B.; Moustafa, E.B.; Alazwari, M.A.; Taha, M.A. An Investigation of the Mechanical, Thermal and Electrical Properties of an AA7075 Alloy Reinforced with Hybrid Ceramic Nanoparticles Using Friction Stir Processing. *Metals* **2023**, *13*, 124. [[CrossRef](#)]
32. Moustafa, E.B.; Melaibari, A.; Basha, M. Wear and microhardness behaviors of AA7075/SiC-BN hybrid nanocomposite surfaces fabricated by friction stir processing. *Ceram. Int.* **2020**, *46*, 16938–16943. [[CrossRef](#)]
33. Rajan, H.B.M.; Dinaharan, I.; Ramabalan, S.; Akinlabi, E.T. Influence of friction stir processing on microstructure and properties of AA7075/TiB<sub>2</sub> in situ composite. *J. Alloys Compd.* **2016**, *657*, 250–260. [[CrossRef](#)]
34. Zhou, X.; Luo, C.; Hashimoto, T.; Hughes, A.E.; Thompson, G.E. Study of localized corrosion in AA2024 aluminium alloy using electron tomography. *Corros. Sci.* **2012**, *58*, 299–306. [[CrossRef](#)]
35. Hou, W.; Oheil, M.; Shen, Z.; Shen, Y.; Jahed, H.; Gerlich, A. Enhanced strength and ductility in dissimilar friction stir butt welded Al/Cu joints by addition of a cold-spray Ni interlayer. *J. Manuf. Process.* **2020**, *60*, 573–577. [[CrossRef](#)]
36. Kumar, S.; Sarma, V.S.; Murty, B.S. Influence of in situ formed TiB<sub>2</sub> particles on the abrasive wear behaviour of Al–4Cu alloy. *Mater. Sci. Eng. A* **2007**, *465*, 160–164. [[CrossRef](#)]
37. Monikandan, V.V.; Jacob, J.C.; Joseph, M.A.; Rajendrakumar, P.K. Statistical Analysis of Tribological Properties of Aluminum Matrix Composites Using Full Factorial Design. *Trans. Indian Inst. Met.* **2015**, *68*, 53–57. [[CrossRef](#)]

38. El-Moayed, M.H.; Shash, A.Y.; Rabou, M.A.; El-Sherbiny, M.G. Thermal-induced Residual Stresses and Distortions in Friction Stir Welds—A Literature Review. *J. Weld. Join.* **2021**, *39*, 409–418. [[CrossRef](#)]
39. Öksüz, K.E.; Bağırov, H.; Şimşir, M.; Karpuzoğlu, C.; Özbölük, A.; Demirhan, Y.Z.; Bilgin, H.U. Investigation of Mechanical Properties and Microstructure of AA2024 and AA7075. *Appl. Mech. Mater.* **2013**, *390*, 547–551. [[CrossRef](#)]
40. Li, J.; Cao, F.; Shen, Y. Effect of Welding Parameters on Friction Stir Welded Ti–6Al–4V Joints: Temperature, Microstructure and Mechanical Properties. *Metals* **2020**, *10*, 940. [[CrossRef](#)]

**Disclaimer/Publisher’s Note:** The statements, opinions and data contained in all publications are solely those of the individual author(s) and contributor(s) and not of MDPI and/or the editor(s). MDPI and/or the editor(s) disclaim responsibility for any injury to people or property resulting from any ideas, methods, instructions or products referred to in the content.